Structural and Motional Heterogeneity in α,ω-Dicarboxylatopolybutadiene: An NMR Study

V. J. McBrierty,[†,‡] D. C. Douglass,[*,‡] X. Zhang,[†] F. X. Quinn,[†] and R. Jérôme[§]

Department of Pure and Applied Physics, Trinity College, Dublin 2, Ireland, AT&T Bell Laboratories, Murray Hill, New Jersey 07974, and Laboratory of Macromolecular Chemistry and Organic Catalysis, University of Liège, Sart-Tilman 4000, Liège, Belgium

Received October 22, 1992; Revised Manuscript Received December 29, 1992

ABSTRACT: NMR relaxation data for α,ω-dicarboxylatopolybutadiene ($\bar{M}_n$ = 4600 and 1900), in the acid and Zr-neutralized forms, illustrate graphically the qualitative features of thermoreversible structural cross-link formation, due to end-group interactions and the concomitant effect on molecular motion. These cross-links are in the form of aggregates in the neutralized telechelic. The precise nature of end-group associations in the acid is less certain, but one can reasonably speculate that dimers or higher multiplets are formed. The ability to resolve end-group carboxyl and proton resonances gives more detailed, though, as yet, incomplete, insight into chain dynamics at the cross-link itself. The temperature dependence of the chemical shift for the acid proton in PBH(1900) is rationalized in terms of a contribution of trace amounts of water in the sample and at least the partial break up of the cross-link above ca. 350 K in PBH(1900). Proton $T_{1\rho}$ data are consistent with this conjecture.

Introduction

Ionomers, formed by the incorporation of small concentrations (<10 mol %) of neutralizable moieties into linear nonpolar chains, exhibit intriguing mechanical and transport properties that differ greatly from those of the neat prepolymer.[1,2] A comprehensive range of experiments points to the development of fluctuating cross-links due to multiple formation of ion pairs in the first instance, developing at higher concentrations (50–100 ion pairs) into larger clusters (10–30 Å in diameter) at distances of 20–100 Å apart or into contiguous regions of overlapping multiplets. As Dreyfus pointed out,[3] the creation of ion pairs involves electrostatic energies that are much greater than the few kT needed to deform a chain segment.

The extent to which ion aggregation occurs depends on numerous factors: prepolymer molecular weight, chain elasticity and flexibility, the extent of entanglements, the polarity of the medium, the nature and concentration of cations, and the degree of neutralization. The location of the ion on the chain is also relevant for steric hindrance effects which can be important in the case of randomly disposed attachments, whereas the incorporation of ionic moieties at both ends of a chain to form a halototelechelic polymer (HTP) can give rise to other effects such as chain entanglements. These HTP systems are generally considered to be suitable model systems for exploring structure/property relationships.

Thermorheological experiments typically demonstrate the importance of ion concentration and type in HTPs.[4-6] In the case of HTPs, multiplet rather than cluster formation is favored.[7] At low concentrations ($\bar{M}_n > 2 \times 10^4$ in polyisoprene (PIP)-based HTP), the ionic end groups cross-link but not in a way that overrides the time-temperature superposition character of backbone chain relaxation.[6] The shift factors obey the Williams–Landel–Ferry (WLF) expression in support of free volume concepts. At higher ion concentration, SAXS reveals the formation of a second, well-separated, phase of ionic domains[7] thought to be made up of thermoreversible cross-links. Relaxation of this phase is Arrhenius rather than WLF in character. The evolution of this three-dimensional cross-linked network is responsible for gel formation in these systems.

Register and co-workers[8] demonstrate the importance of cation types in neutralized PIP-based HTP. Of the systems studied, Ca^{2+} and Sr^{2+} telechelics have the highest small-strain tensile moduli arising in part from interlocking loops. Strain hardening is observed in Ca^{2+} and Ni^{2+} ionomers for which EXAFS reveals more cohesive and highly ordered ionic microdomains: structural breakdown occurs when the interlocking loops or entanglements become taut. For Sr^{2+}-, Zn^{2+}-, and Cd^{2+}-neutralized polymer, stressed entanglements can relax by extracting chain ends out of the aggregates, a process known as ion-hopping.

Experiments such as EXAFS,[8,9] ESR,[10,11] NMR,[12-14] ENDOR,[15] Mössbauer,[16-18] excimer fluorescence,[19] and dielectric relaxation[20] can delineate events in the immediate vicinity of the cation from those on a larger dimensional scale[21-26] from which it is clear that cross-links involve both physical and chemical attachments. Recall too the analogy drawn between ionomers and carbon black filled elastomers regarding behavior in the immediate vicinity of the filler.[27] Specifically, it was argued, but not unequivocally demonstrated,[13] that chains anchored in aggregates of multiplets or clusters are constrained in a fashion similar to immobilized polymer detected in the filled elastomer. Because of the relatively small amount of material involved, its direct observation is illusive and remains undetected in the routine determination of T_g, for example by DSC. This concept of motionally constrained chains with a concomitantly higher T_g in the immediate vicinity of multiplets or clusters forms the basis of a recent model proposed by Eisenberg and co-workers[28] which, additionally, envisages the progressive development of regions of restricted mobility arising from overlapping multiplets at high ionic concentrations.

Of course, the degree to which backbone polymer is constrained will depend on the degree of cohesion of the aggregate and the extent to which it is in a state of structural dynamic equilibrium as evidence, for example, by ion-hopping between aggregates.[8,25] An early observation by Pineri and co-workers[10] on Cu^{2+}-neutralized polybutadiene/methacrylic acid ionomer is noteworthy in that the appearance of a dynamic mechanical relaxation

---

[†] Trinity College.
[‡] AT&T Bell Laboratories.
[§] University of Liège.

0024-9297/93/2226-1734$04.00/0

peak at 340 K upon neutralization and the disappearance of the ESR signal for Cu^{2+}–Cu^{2+} pairs as the temperature is increased are assigned to the reversible dissociation of ion pairs.

The purpose of this paper is to exploit the site-specific character of high-resolution solid-state ^1H and ^{13}C NMR, with molecular weight and temperature as disposable parameters, in order to examine further the events in the vicinity of aggregates in neutralized and unneutralized carboxy-terminated polybutadiene telechelics. The thrust of the paper will be to examine the dynamics of the telechelic chain and, in particular, the end groups which participate directly in cluster formation. Structural information will be elicited where possible.

Experimental Section

Proton spectra were obtained in Bruker spectrometers operating at 400, 300, and 40 MHz, respectively. High-resolution data were recorded under MAS conditions with typical spinning frequencies at 3.5–4.0 kHz. MAS carbon spectra were recorded at 75.4 MHz with CW proton decoupling (B_1 = 5–10 G) and with either cross polarization or use of a single 90° pulse. The 180°–τ–90° inversion–recovery sequence without decoupling provided $T_1(^{13}C)$. Proton $T_{1\rho}$ measurements (at ν_0 = 300 MHz) were performed with a locking pulse field strength of 10 G. Low-resolution T_2 measurements utilized 90° pulses for $T_2 < 50$ μs and the 90°–τ–180° spin–echo sequence thereafter.

Two samples of α,ω-dicarboxylatopolybutadiene were used in this study:

(1) A sample (Hycar CTB 2000 × 156) commercialized by B. F. Goodrich, with molecular characteristics as follows: $\bar{M}_n$ = 4600; $\bar{M}_w/\bar{M}_n$ = 1.8; functionality = 2.01; cis/trans/vinyl ratio = 20/65/15.

(2) A sample (Nisso-PB C-1000) from Nippon Co. (Japan), with molecular characteristics as follows: $\bar{M}_n$ = 1900, assuming two acid groups per chain; $\bar{M}_w/\bar{M}_n$ = 1.23; the material contained vinyl units.

Samples were neutralized with zirconium isopropoxide under carefully controlled conditions. A 5 wt % solution of the carboxy-telechelic polybutadiene was prepared in toluene previously dried by refluxing over calcium hydride. The polymer was then dried by three successive azeotropic distillations of toluene, and an appropriate amount of zirconium isopropoxide (0.1 mol L^{-1} solution in toluene) was added to the final 5 wt % solution of the polymer. Zirconium alkoxide was used in an alkoxide/acid molar ratio of 6, that is, to a degree of neutralization of 600%. The neutralization reaction was driven to completion by azeotropic distillation of the isopropyl alcohol fromed as a reaction byproduct. When ca. 20% of the toluene volume was distilled off under reduced pressure, it was replaced by fresh solvent and a further distillation run was carried out. After three such runs, 20% of the distilled toluene was replaced by toluene saturated by water in order to hydrolyze the unreacted zirconium alkoxide functions. Again three distillation runs were effected under these conditions. Toluene was finally distilled off completely and the polymer dried to constant weight under vacuum at 65 °C. The samples contained 1 wt % of Irganox 1010 antioxidant. By their nature, it is likely that all samples contained trace amounts of water.

The choice of Zr to neutralize the acid relies upon the unique properties of the parent cation. It is a tetravalent transition metal which forms more covalent bonds with carboxylates than the more commonly used alkaline and alkaline-earth cations. A noticable cross-linking effect is promoted when an excess of zirconium alkoxides is used in the neutralization of the chain acid end groups and subsequently hydrolyzed. The chain network is then stabilized by carboxylatozirconium oxohydroxide groups which behave as small inorganic domains of a much greater cross-linking efficiency and stability toward polar compounds compared to the alkaline and alkaline-earth telechelics. Problems encountered with iron as a neutralizing cation[13] do not arise with Zr which is nonparamagnetic.

Acid and neutralized samples are designated PBH($\bar{M}_n$) and PBZr($\bar{M}_n$), respectively; the number-average molecular weight is denoted in parentheses in each case. The study also included a sample terminated with phenyl groups (Scientific Polymer Products, No. 437; $\bar{M}_n$ = 2600, 50% vinyl, 25% trans-1,4, and 99% saturated) which does not cluster.

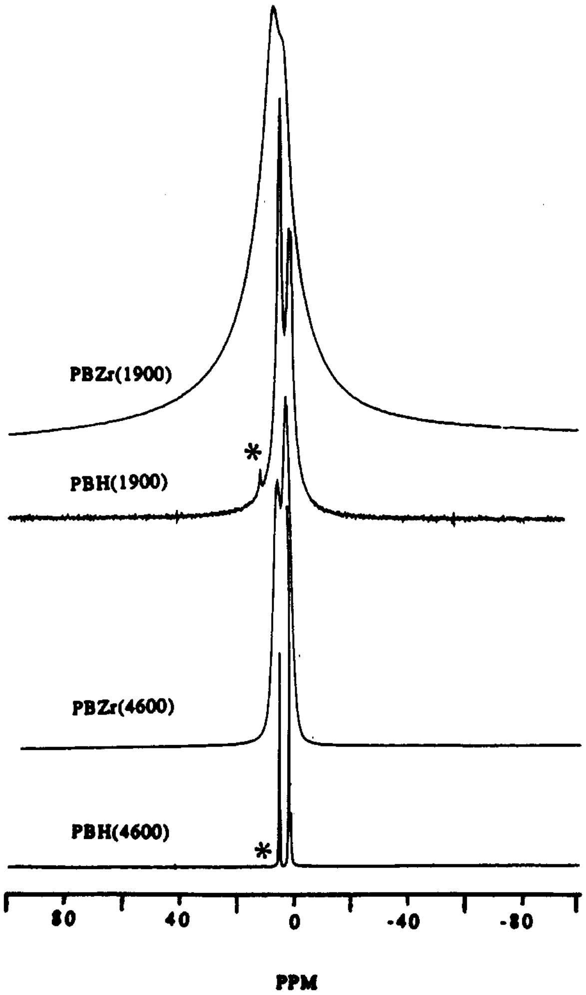

Figure 1. 400-MHz ^1H spectra for PBH(1900), PHZr(1900), PBH(4600), and PBZr(4600). Variations in CH_2 and CH peak height intensities reflect the different tacticities in PB(2000) and PB(4600). The acid protons, denoted with asterisks, are just detectable in PHB(4600).

Results and Discussion

General Observations. Because of the site-specific character of high-resolution NMR, it is possible to delineate end-group behavior from the more general motions of the butadiene chain above its glass transition. Data analysis will first address the overall NMR response which yields a qualitative but nonetheless informative picture of the chain dynamics of the telechelic.

Consider the 400-MHz proton spectra for neutralized and unneutralized polymers (Figure 1). Typically, the spectrum for PBH(1900) reveals the usual CH_2, CH, and COOH contributions at progressively higher chemical shifts. Resolution of the carboxylate proton signal, though less clear in PBH(4600), permits direct examination of end groups and their primary role in multiplet formation in the acid.

Line broadening reflects the enhanced motional constraints of both a spatial and temporal nature induced by neutralization which are consistent with the creation of stronger cross-links in the neutralized telechelic. The formation of the high-temperature plateau in the $T_2(^1H)$ versus temperature data for PBZr(4600) (Figure 2) is also typically consistent with this scenario, as observed earlier in other systems.[13] The appearance of two T_2 components

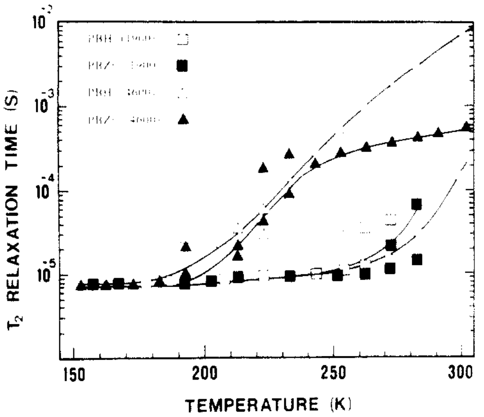

Figure 2. 40-MHz $T_2(^1H)$ data for the four samples indicated. The lines are drawn through the data points for clarity of presentation.

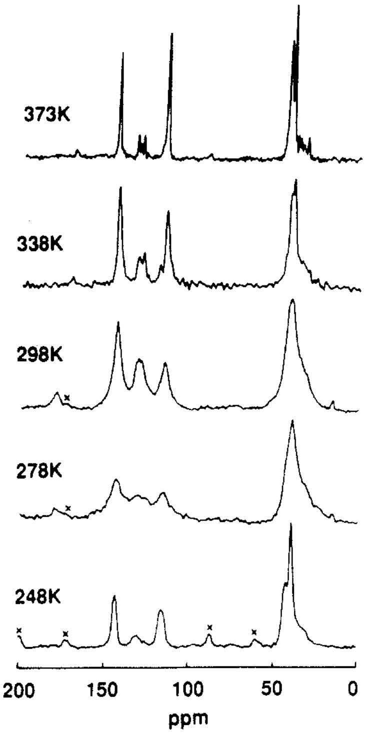

Figure 3. 75.4-MHz ^{13}C CPMAS spectra of PBZr(1900) at the temperatures indicated. Spinning sidebands are denoted by ×.

over a broad temperature range which increase in tandem with increasing temperature is typical of systems undergoing broadly distributed and cooperative motions as, indeed, might be expected in the materials under current examination.

The PB backbone chain is less constrained in the higher molecular weight PBZr(4600) telechelic compared with PBZr(1900). Line narrowing in PBZr(1900) with increasing temperature is revealed both in the proton spectra of Figure 2 and in the ^{13}C spectra portrayed in Figure 3. That ^{13}C spectra at higher temperatures for PBZr(1900) are similar to those for the unneutralized telechelic at room temperature (Figure 4) offers preliminary evidence for thermoreversible cross-links. Not surprisingly, the change is less pronounced in PBZr(4600) since backbone motions are already quite extensive at room temperature.

It is interesting to compare spectra for PBH(4600), PBH(1900), and polybutadiene terminated with phenyl groups, PBPh(2600), for which the formation of cross-links is not expected (Figure 5). The peaks for PBPh(2600) are well resolved as anticipated for an un-cross-linked polymer well above its glass transition. In contrast, there is a progressively greater degree of peak overlap in PBH(4600) and PBH(1900) which is again indicative of the motional constraint due to cross-linking even in the acid forms of the telechelic. Note, in passing, that experimental and theoretical peak intensities in these spectra agree to within 10% or less, which confirms the accuracy of peak assignments and the molecular weight characterization.

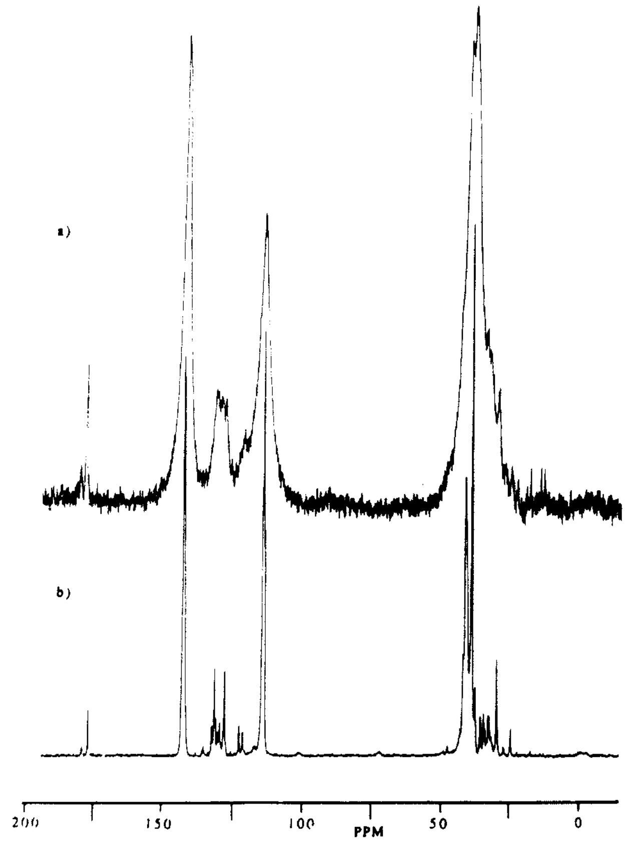

Figure 4. 75.4-MHz ^{13}C MASDD spectra for PBH(1900) observed by a single 90° pulse at (a) 297 and (b) 362 K.

Peak resolution is significantly better in ^{13}C MAS spectra compared with proton spectra, particularly at elevated temperatures. Additionally, ^{13}C resonance can monitor chain end groups in the neutralized telechelic. Comparison of ^{13}C spectra for PBZr(1900) and PBH(1900) in Figures 3 and 4 reveals appreciable broadening of the C*OO carbon peak upon neutralization.

At this juncture a number of interim conclusions may be drawn:

(1) Aggregation occurs in the neutralized telechelic.

(2) While the precise nature of end-group associations in the acid is less certain, the formation of dimers[29] or higher multiplets is most likely.

(3) The network gel thus formed is stronger in the neutralized material than in the acid.

(4) The similarity of spectra for PBZr(1900) at high temperatures with room-temperature spectra for PBH(1900) in which clustering is weaker offers preliminary evidence for thermoreversible cross-links.

Localized Behavior at the Clusters. As discussed above, the behavior of the carboxylate carbon, and proton in the case of the acid, probes events at the structural cross-link since the carboxylate group participates directly in their formation. Chemical shift versus temperature reflects changes in the local environment and motional dynamics of the end groups. Thus, the observed upfield shift in the C*OO carbon resonance with increasing temperature (Figure 3) may be due (i) to the progressive dehydration of the carboxylate moiety, assuming that the

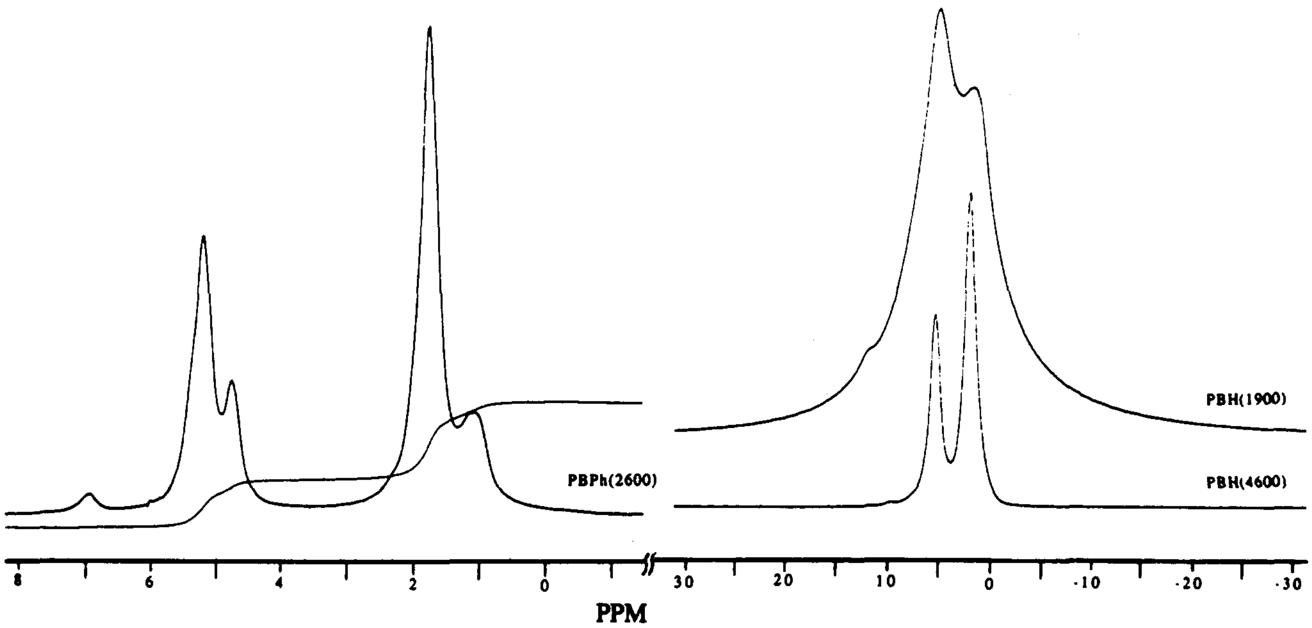

Figure 5. Comparison of proton spectra for PBH(1900), PBH(4600), and PB terminated with phenyl groups, PBPh(2600), for which cross-links are not expected.

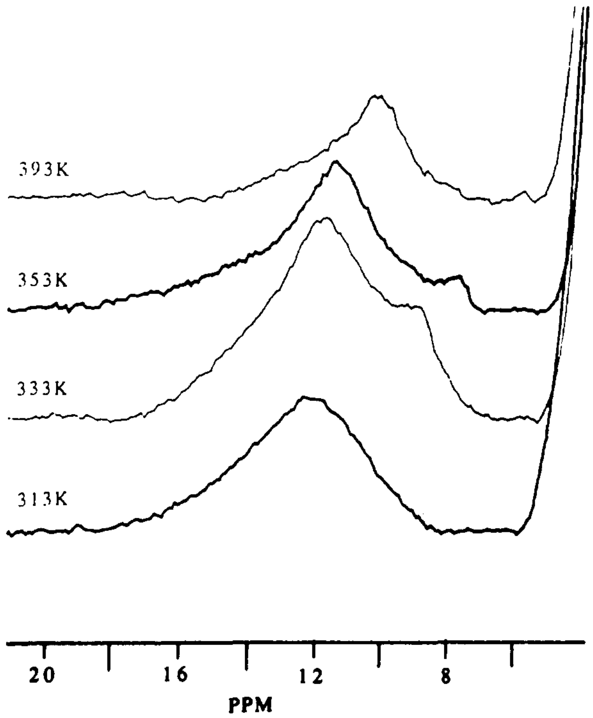

Figure 6. Behavior of the acid carboxylate proton in PBH(1900) as a function of temperature.

samples are not completely dry, (ii) to dissociation of ionic interactions, and/or (iii) to a change in the molecular motional or structural environment of the end group. For the acid telechelics, an upfield shift would accompany the progressive dissociation of hydrogen bonds. Clearly it is not possible at this juncture to delineate between these possibilities until controlled hydration experiments are carried out. These experiments are underway.

The acid proton spectral region for selected temperatures between 313 and 393 K (Figure 6) reveals additional insight into events at the end-group complex. Owing to the low intensity of the acid proton relative to the nearby methine absorptions, this spectral region has a rapidly changing base line and the weak resonance appears as a shoulder on a large but relatively smooth section of the stronger line. This sloping base line was removed instrumentally using a spline fit procedure to record the spectra as reported. In the 333–353 K range, an interesting structural feature develops on the low-frequency side of the acid proton absorption. This smaller though fairly well-resolved absorption shifts to lower frequency more rapidly than the main acid proton absorption as the temperature is increased and appears to join the methine line near 393 K. The direction of the shifts of both the main acid proton line and the smaller feature with increasing temperature is consistent with that expected from the dissociation of water and ions as observed in the dilution studies of, say, acetic acid in CCl_4 at concentrations where structures more complex than dimers are thought to be present.[30] It is assumed that dilution and increasing temperature have similar effects. It remains to be seen in subsequent hydration experiments whether or not the low-frequency absorption results from water that has moved into an environment dominated by polymer chains as opposed to partially ionic clusters of carboxyl groups and water. In brief, the slight narrowing and the shift of the acid proton absorption are consistent with the expectation that the aggregates at least partially break up in the 350–390 K temperature range.

This break up is more evident in the temperature dependence of $T_{1\rho}(^1H)$. Figures 7 and 8 compare $T_{1\rho}$ for the total proton signal for both sets of acid and Zr-neutralized samples. Each signal can be resolved into fast, $T_{1\rho s}$, and slower, $T_{1\rho L}$, decaying components. The large scatter in $T_{1\rho s}$ arises from its relatively small amplitude which is typically less than 10%. The minimum in $T_{1\rho s}$ in the acid samples near 360 K is presumed to reflect the dissociation of end-group complexes which is in accord with the scenario outlined above. Indeed, the rather sharp $T_{1\rho s}$ minimum in PBH(1900) is reminiscent of a first-order structural transition. The broadening of the $T_{1\rho s}$ minimum and its shift to higher temperatures upon neutralization (beyond the temperature range of measurement in the case of PBZr(1900) are consistent with the formation of a more tenacious network of aggregates in the neutralized material.

Returning again to the ^{13}C data for PBH(1900) in Figure 4, note that the carboxyl carbon resonance is split into a subsidiary and a main, lower frequency, peak. It is likely that the two-component lines reflect different carboxyl

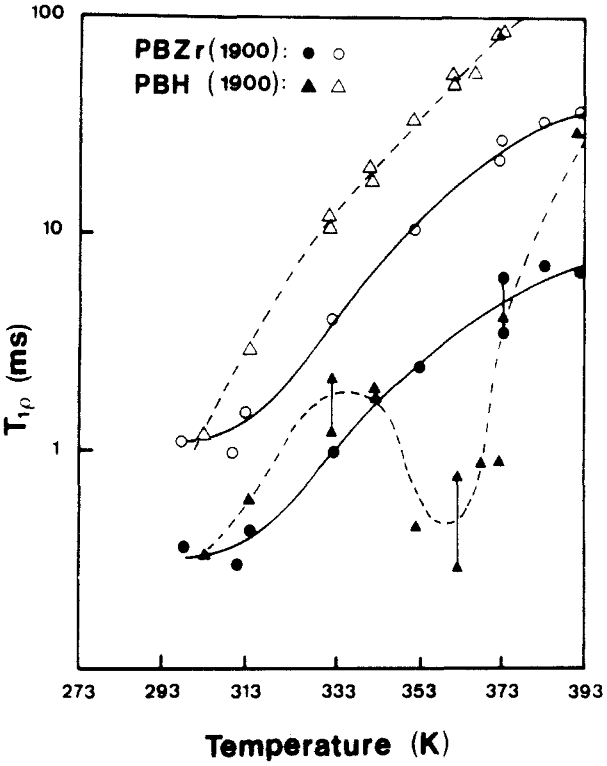

Figure 7. $T_{1\rho}(^1H)$ for PBH(1900) and PBZr(1900) as a function of temperature.

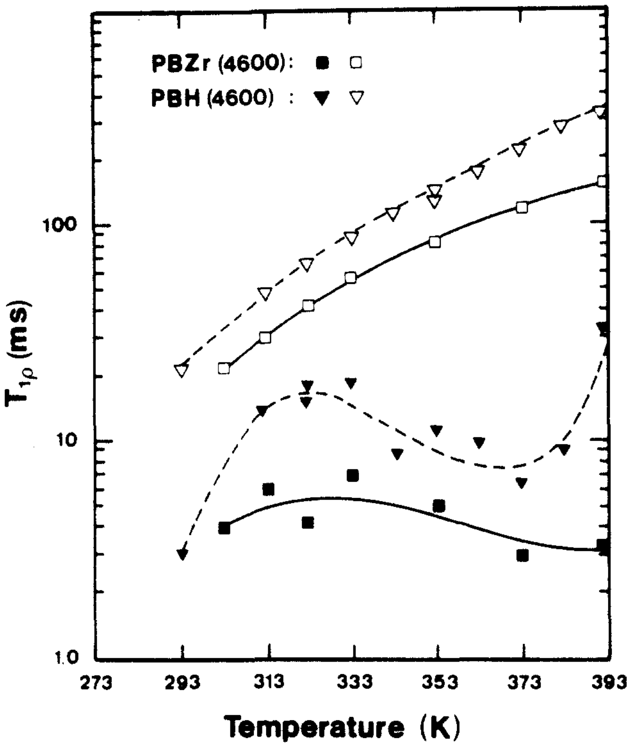

Figure 8. $T_{1\rho}(^1H)$ for PBH(4600) and PBZr(4600) as a function of temperature.

carbon environments, perhaps arising from preferential levels of hydration. Recall that this chemical shift in anhydrous oxalic acid is 162 ppm compared with 163 ppm for oxalic acid dihydrate.[30] The two-component line does, however, transform into a single broadened line upon neutralization which is consistent with this viewpoint and also with the interpretation of a more rigid aggregate in the neutralized telechelic.

Spin-lattice relaxation measurements do not cast much light on chain dynamics in the vicinity of the aggregate.

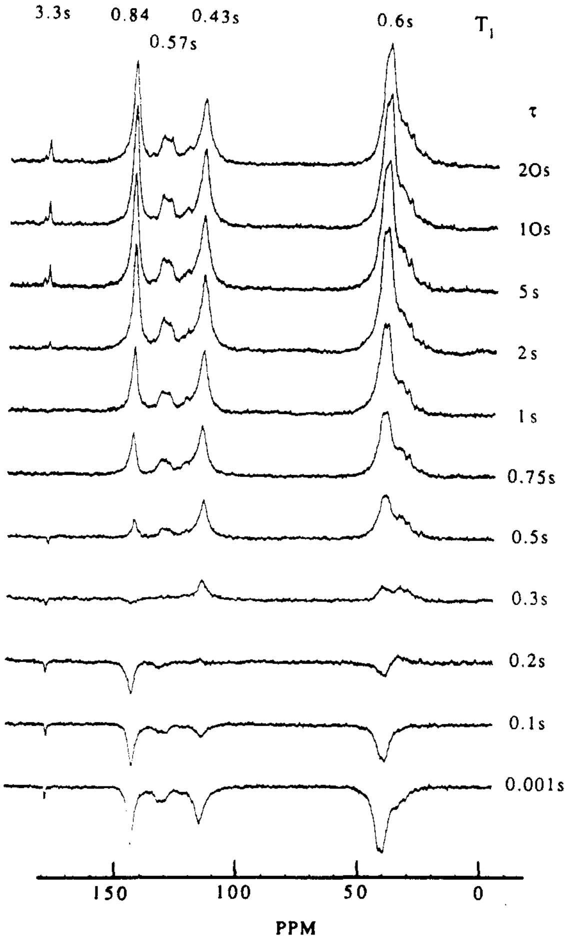

Figure 9. 75.4-MHz ^{13}C spectra for PBH(1900) recorded under the inversion-recovery sequence, 180°–τ–90°, for various delay times τ. T_1 for resolved resonances are as indicated.

The predicted T_1 values for the methylene and methine carbons determined from ^{13}C inversion-recovery spectra for PBH(1900) (Figure 9) are consistent with magnitudes expected for the number of attached protons in each case which no more than confirms the spectral line assignments. That T_1 is long (3.3 s) for the carboxyl carbon is also to be expected for a carbon without a directly attached proton. Unfortunately, the carboxyl carbon resonance for PBZr(1900) was too weak to obtain meaningful T_1 relaxation data, thereby precluding comparison with the unneutralized material.

In summary, end-group behavior is generally consistent with the notion of ionic structural cross-links that are in a state of dynamic equilibrium and prone to thermoreversible cross-link formation. As the temperature increases, main-chain motions become increasingly vigorous and, at sufficiently high temperatures, they can overcome the binding energies which hold the cluster together. There is preliminary evidence of hydration effects in the nominally dry material. Hydration effects are exceedingly important in the vicinity of the end-group complexes, and these will be examined in a controlled way in a subsequent study.

Conclusions

NMR relaxation data for acid and Zr-neutralized α,ω-dicarboxylatopolybutadiene telechelics ($\bar{M}_n$ = 4600 and 1900) illustrate graphically the qualitative features of structural cross-links involving chain end groups and their effect on molecular motion. The ability to resolve carboxyl resonances gives more detailed, though incomplete, insight into chain dynamics at the cross-link itself where, for example, there is evidence of the thermoreversibility of cross-link formation. The temperature dependence of the chemical shift for the acid proton in PBH(1900) is rationalized in terms of a contribution of trace amounts of water in the sample and at least the partial breakup of the cross-link below 360 K in PBH(1900). Proton $T_{1\rho}$ data and the behavior of the carboxyl carbon are consistent with this conjecture.

References and Notes

(1) Pineri, M., Eisenberg, A., Eds. *Structure and Properties of Ionomers*; Reidel: Dordrecht, The Netherlands, 1987.
(2) MacKnight, W. J.; Earnest, T. R., Jr. *Macromol. Rev.* **1981**, *16*, 41.
(3) Dreyfus, B. *Macromolecules* **1985**, *18*, 284.
(4) Broze, G.; Jérôme, R.; Teyssié, Ph. *Macromolecules* **1981**, *14*, 224; **1982**, *15*, 920; **1982**, *15*, 1300.
(5) Broze, G.; Jérôme, R.; Teyssié, Ph. *J. Polym. Sci., Polym. Phys.* **1983**, *21*, 2205.
(6) Broze, G.; Jérôme, R.; Teyssié, Ph.; Marco, C. *Macromolecules* **1983**, *16*, 996; **1983**, *16*, 1771.
(7) Williams, C. E.; Russell, T. P.; Jérôme, R.; Horrion, J. *Macromolecules* **1986**, *19*, 2877.
(8) Register, R. A.; Foucart, M.; Jérôme, R.; Ding, Y. S.; Cooper, S. L. *Macromolecules* **1988**, *21*, 1009.
(9) Jérôme, R.; Vlaic, G.; Williams, C. E. *J. Phys. (Lett.)* **1983**, *44*, L-717.
(10) Pineri, M.; Meyer, C.; Levelut, A. M.; Lambert, M. *J. Polym. Sci., Polym. Phys.* **1974**, *12*, 115.
(11) Schlick, S.; Alonzo-Amigo, M. G. *Macromolecules* **1989**, *22*, 2634.
(12) Mauritz, K. Hora, C. J.; Hopfinger, A. J. *Adv. Chem. Ser.* **1980**, *187*, 123.
(13) McBrierty, V. J.; Smyth, G.; Douglass, D. C. Reference 1, p 149.
(14) Boyle, N. G.; McBrierty, V. J.; Douglass, D. C. *Macromolecules* **1983**, *16*, 75.
(15) Schlick, S.; Sjoqvist, L.; Lund, A. *Macromolecules* **1988**, *21*, 535.
(16) Rodmacq, B.; Pineri, J.; Coey, J. M. D. *Rev. Phys. Appl.* **1980**, *15*, 1179.
(17) Meagher, A.; Smyth, G.; McBrierty, V. J.; Coey, J. M. D.; Pineri, M. *J. Chem. Phys.* **1985**, *83*, 2552.
(18) Meagher, A.; Coey, J. M. D.; Belakhovsky, M.; Pineri, M.; Jérôme, R.; Vlaic, G.; Williams, C.; Dang, N. V. *Polymer* **1986**, *27*, 1979.
(19) Granville, M.; Jérôme, R.; Teyssié, Ph.; DeSchryver, F. C. *Macromolecules* **1988**, *21*, 2894.
(20) Yano, S.; Tadano, K.; Jérôme, R. *Macromolecules* **1991**, *24*, 6439.
(21) Moudden, A.; Levelut, A. M. *J. Polym. Sci., Polym. Phys.* **1977**, *15*, 1707.
(22) Broze, G.; Jérôme, R.; Teyssié, Ph.; Gallot, B. *J. Polym. Sci., Polym. Lett.* **1981**, *19*, 415.
(23) Chu, B.; Wu, D.; MacKnight, W. J.; Wu, C.; Phillips, J. C.; LeGrand, A.; Lautman, C. W.; Lunberg, P. D. *Macromolecules* **1988**, *21*, 523.
(24) Wu, D. Q.; Phillips, J. C.; Lundberg, R. D.; MacKnight, W. J.; Chu, B. *Macromolecues* **1989**, *22*, 992.
(25) Mauritz, K. A.; Fu, R.-M. *Macromolecules* **1988**, *21*, 1324.
(26) Mauritz, K. A.; Yun, H. *Macromolecules* **1988**, *21*, 2738.
(27) O'Brien, J.; Cashell, E.; Wardell, G. E.; McBrierty, V. J. *Macromolecules* **1976**, *9*, 653.
(28) Eisenberg, A.; Hird, B.; Moore, R. B. *Macromolecules* **1990**, *23*, 4098.
(29) Schlick, S., private communication.
(30) Griffin, R. G.; Pines, A.; Pausak, S.; Waugh, J. S. *J. Chem. Phys.* **1975**, *63*, 1267.